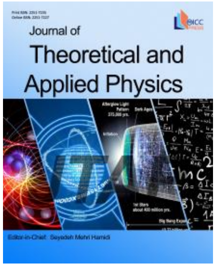

J. Theor. Appl. Phys., 2026; 20(5): 482-494

Journal of Theoretical and Applied Physics
(JTAP)

https://doi.org/10.57647/jtap.2026.2005.01

Research Article

Analysis of Electromagnetic Scattering from Double Metallic Rods Covered by Anisotropic Inhomogeneous Plasma via FE-BI Method

Anis Soltani[1], Zeinab Rahmani*[1], Ebrahim Heidari Semiromi[2]

[1]*Department of Laser and Photonics, Faculty of Physics, University of Kashan, Kashan, Iran*
[2]*Department of Condensed Matter, Faculty of Physics, University of Kashan, Kashan, Iran*

***Corresponding author:** z.rahmani@kashanu.ac.ir

Article History:

Received:
22 October 2025

Revised:
01 December 2025

Accepted:
23 April 2026

Published in Issue:
31 October 2026

©2026 the Author(s). Published by the OICC Press under the terms of the © CC BY 4.0, Creative Commons Attribution License, which permits use, distribution and reproduction in any medium, provided the original work is properly cited.

Abstract

We investigate the scattering of linearly polarized plane electromagnetic waves from a system of two metallic cylinders covered by non-uniform plasma layers, using the Finite Element–Boundary Integral (FE-BI) method. The structure can be regarded as a plasma antenna. To better reflect practical conditions, we consider inhomogeneous plasma covers, since laboratory and atmospheric plasmas are typically non-uniform. Introducing anisotropy and inhomogeneity in the plasma coating enhances the tunability and flexibility of the radar cross-section (RCS). We analyze the total axial magnetic field, the RCS, and the backscattering RCS (BRCS) under variations of incidence angle, wavelength, polarization, external DC magnetic field, and plasma inhomogeneity. For comparison, the system is also examined without plasma coating and without magnetic field, to highlight the role of anisotropic inhomogeneous plasma layers. The validity of the FE-BI method is confirmed by benchmarking our results against the Perfectly Matched Layer (PML) technique.

Keywords: Electromagnetic waves, Inhomogeneous plasma, Anisotropic plasma, Radar cross-section, FE-BI method, External magnetic field

Cite this article: Soltani A., Rahmani Z., Heidari Semiromi E., Analysis of electromagnetic scattering from double metallic rods covered by anisotropic inhomogeneous plasma via FE-BI method. J Theor Appl Phys. 2026; 20(5):482-494. https://doi.org/10.57647/jtap.2026.2005.01

1. Introduction

In practical applications, scattering is an interesting and important process [1–4]. The scattering of plane electromagnetic waves from different structures has been investigated by many researchers. When EM waves incident to a target, they interact with it, and the ratio of the energy of the scattered wave to the energy of the incident wave can indicate the existence of the target. Although the internal structure and characteristics of the target cannot be fully recognized from this ratio, the scattering pattern can roughly determine the size and geometry of the target. In the past, three-dimensional scattering from infinite homogeneous anisotropic circular cylinders was investigated analytically and numerically [5–7]. Adey studied scattering of a plane electromagnetic wave by coaxial dielectric cylinders [8]. In recent years, plasma has attracted the attention of many researchers due to its application potentials in communication, medicine, optics, defense technology, stealth, and the design of plasma antennas [9–13]. Plasma antennas are lightweight, compact, and reconfigurable during operation.

If the plasma is turned off, the antenna exhibits a low radar cross section, making it difficult to detect by radar, which is advantageous for stealth. When the gas confined in the chamber is ionized, the plasma acts as a conductor that reflects or transmits electromagnetic signals for communication purposes [14, 15]. In addition, plasma antennas offer considerable flexibility and adjustability due to many variable parameters such as plasma frequency, collision frequency, cyclotron frequency, and plasma temperature. Scattering from a cylinder covered with an inhomogeneous dielectric sheath has also been investigated [16, 17]. However, due to the importance of this subject, research on scattering by cylinders covered with other materials, including plasma, is ongoing [18], [19]. The scattering of electromagnetic waves by plasma spheres was reported in [20]. The scattering from a fully electrically conductive cylinder with an anisotropic plasma coating was considered by Ghaffar et al. [21]. Studies on reducing radar cross-section or cloaking have become important topics in recent years [22, 23]. Concealment by plasma coating is well known as a method to decrease radar cross-section. In this process, the radar wave is weakened when colliding with the charged particles of the plasma layer covering the structure, and the intensity of the return wave is reduced. Adjusting plasma layer characteristics can further improve RCS reduction [18]. Generally, it is accepted that an anisotropic cylinder with plasma coating is the simplest and most suitable model for rocket re-entry into the Earth's atmosphere. When cylindrical and spherical metallic structures such as missiles and satellites enter the atmosphere, they are immersed in ionospheric plasma. This plasma sheath can be modeled as an inhomogeneous plasma layer around perfectly conducting objects [24, 25]. When these plasma-coated structures are exposed to an external magnetic field such as the Earth's magnetic field, they can be modeled as conducting structures with a magnetized plasma cover [26, 27]. To better understand the radiation process in a cylindrical plasma antenna and to build such an antenna, it is necessary to determine the dependence of surface wave energy conversion coefficients on plasma density inhomogeneity. The non-uniformity of plasma density is an important subject in calculations because it influences antenna performance. Results of studies on planar and cylindrical plasma antennas with large longitudinal irregularity in plasma density are presented in [28, 29].

Unlike previous studies [18, 19, 21] that mainly considered single cylinders or homogeneous plasma coatings, the present work addresses a double-rod metallic structure covered by radially varying anisotropic plasma layers. This configuration introduces additional coupling effects between the rods and highlights how plasma inhomogeneity combined with an external magnetic field can be exploited to control scattering. Therefore, the study provides new insights into both the reduction and enhancement of radar cross-section, extending the applicability of FE-BI methods to more realistic plasma antenna and stealth scenarios. In addition to classical studies, recent reviews and experimental works have highlighted the rapid progress in plasma antenna technology. Magarotto et al. [33] provided a comprehensive review of gaseous plasma antennas, emphasizing their reconfigurability and stealth potential. Pantod [34] discussed analytical solutions of nonlinear differential-difference equations, which are relevant to advanced mathematical modeling approaches used in plasma scattering problems. The dispersion characteristics of plasma-filled cylindrical waveguides [36] and proton-driven plasma wakefield generation [37] are also areas of active research, further illustrating the diverse phenomena and applications within plasma physics. Additionally, research into the plasma effect in tape helix traveling-wave tubes [38] and plasmon resonance coupling in cold overdense dissipative plasma [39] demonstrates the ongoing exploration of complex plasma interactions. Kumar et al. [35] investigated plasma-sprayed Fe-based amorphous/nanocrystalline coatings, showing their mechanical and corrosion resistance properties relevant to plasma-based applications.

These updated references demonstrate that plasma antennas and plasma coatings remain an active and evolving research field, complementing the present analysis. The purpose of this work is to calculate the scattered fields, radar cross section (RCS), and backscattering radar cross section (BRCS) of a system consisting of two metallic cylindrical rods covered by non-uniform plasma layers, where the plasma density varies radially. A constant magnetic field is assumed along the structure axis, which makes the plasma permittivity tensor anisotropic.

2. Geometry and formalism

As we see in Figure (1), two metallic rods with similar radiuses a and the distance d between their centers are situated along the z-axis. Each rod has been covered with an inhomogeneous anisotropic plasma layer whose density $n(\boldsymbol{r})$ is given as follows;

$$n(\boldsymbol{r}) = n_0(1 - \beta\frac{(|\boldsymbol{r} - \boldsymbol{r}_i| - a)^2}{L^2})$$
$$a \le |\boldsymbol{r} - \boldsymbol{r}_i| \le a + L \tag{1}$$

where $\boldsymbol{r}_i$ with $i = 1,2$ represents the position vector of the center or right and left rods, respectively.

10.57647/jtap.2026.2005.01

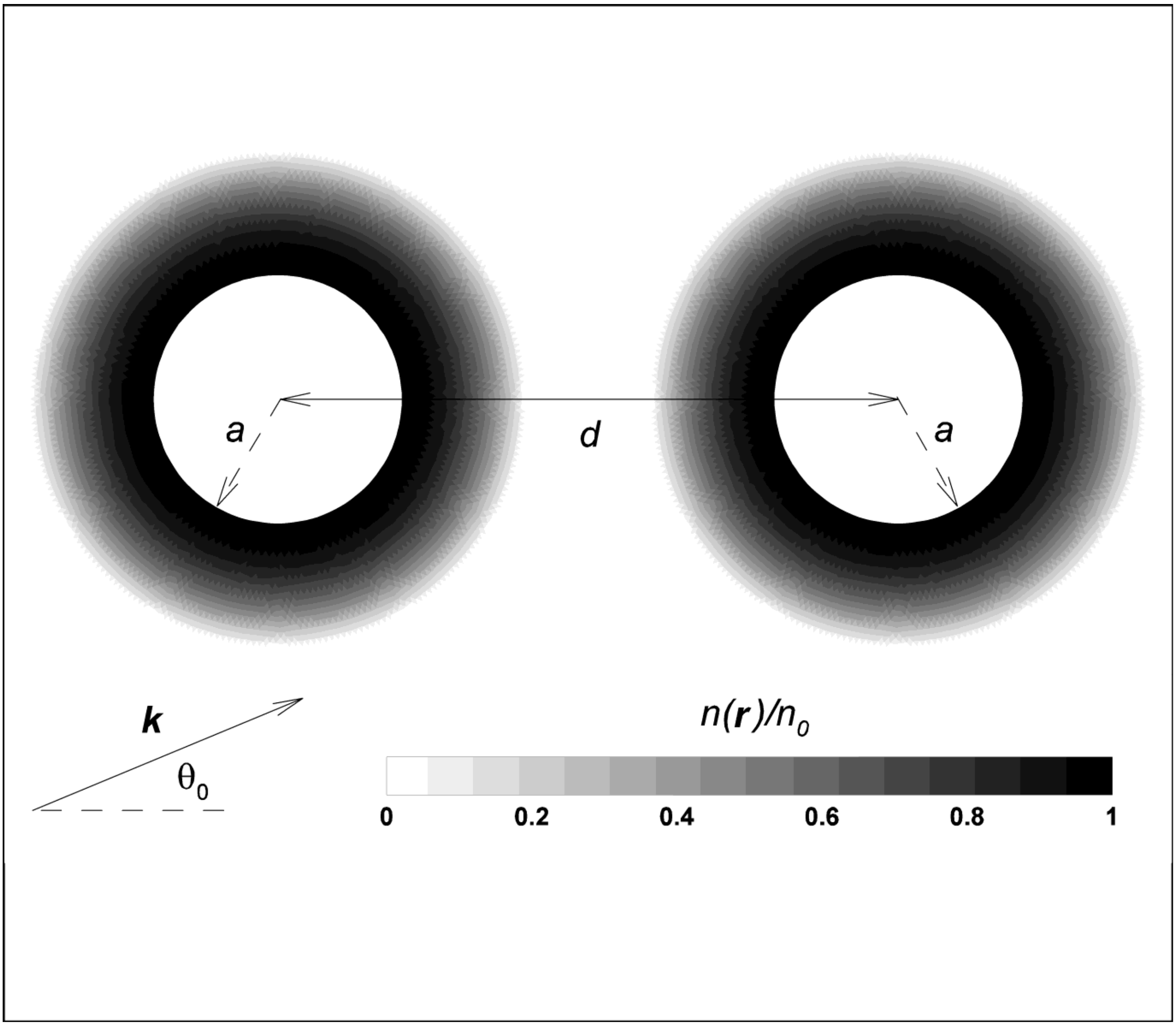

Figure 1. Cross-sectional view of system including two metal cylinders covered by radially inhomogeneous plasma layers located in DC magnetic field H_0

We consider two situations: one with $\beta = 0$ which shows a constant plasma density n_0 along thickness L around each rods after which $n(\boldsymbol{r})$ decreases abruptly to zero, and another situation with $\beta = 1$ which shows that the plasma density decreases radially around each rods from n_0 on the surface of the rod and reaches zero along the thickness L.

It should be noted that in this study, the plasma is modeled as a cold, collisionless medium. This assumption is justified by comparing the characteristic frequency scales of the system. For the microwave regime considered here ($f \approx 10\, GHz$, i.e., $\omega \approx 6 \times 10^{10}\, rad/s$) and typical low-pressure laboratory conditions ($10^{-3} - 1\, Torr$), the electron-neutral collision frequency (ν) is approximately 10^7 Hz. Consequently, the damping ratio is very small ($\nu / w \approx 10^{-4}$ to 10^{-3}), meaning that collisional effects have a negligible impact on the scattering patterns in the first approximation. While collisions can broaden resonances and slightly reduce peak RCS values, neglecting them allows us to isolate and clearly demonstrate the effects of anisotropy and inhomogeneity on RCS control.

This Double metallic rod system is irradiated by a plane electromagnetic wave with TE polarization. The z-component of magnetic field of the incident wave is (for TM polarization just replace $H_z \longrightarrow E_z$):

$$H_z^{\text{in}} = H e^{ik(x\cos\theta_0 + y\sin\theta_0)} \tag{2}$$

Eq. (2) expresses the incident plane wave in Cartesian coordinates. For consistency with the cylindrical geometry of the rods, this expression can be rewritten in cylindrical coordinates (r, φ) as $H_z^{in} = H\, e^{ikr\cos(\varphi - \theta_0)}$. This representation ensures that the incident wave is properly mapped onto the cylindrical system, and the dispersion relation is derived under this coordinate transformation. This mapping is important because the scattering problem is solved in cylindrical coordinates, and the plane wave excitation must be expressed accordingly.

where H is the amplitude, θ_0 is the direction of incidence, and k is the wave number. The amplitude of the corresponding electric field is equal to $E = ZH$ where $Z = \sqrt{\mu_0/\varepsilon_0}$ is the vacuum impedance. In order to calculate the z-component of the scattered wave field, the following boundary integral is used:

$$H_z^{sc} = \oint_C dl' \left(H_z(r')n' \cdot \nabla' G(r,r') - G(r,r')n' \cdot \nabla' H_z(r')\right) \tag{3}$$

where C is a fictitious circular boundary with radius $R = d/2 + a + L$, and the Green's function defined in the $r > R$ area is

$$G(r,r') = \frac{\mathrm{i}}{4}\mathcal{H}_0^{(1)}(k|r - r'|) \qquad r > R \tag{4}$$

It is worthy to note that we have used the Hankel function of the first type because of the phase sign convention $e^{-\mathrm{i}\omega t}$ in our formalism. The boundary integral equation, i.e. Eq. (3), relates the scattered wave field H_z^{sc} to the total field $H_z = H_z^{\mathrm{in}} + H_z^{\mathrm{sc}}$ and its normal derivative on the fictitious boundary. For the region S surrounded by the fictitious boundary C, i. e. the region inside the circular boundary with radius R, we must solve the following two-dimensional boundary value problem to obtain the total field H_z;

$$\nabla\varepsilon^{-1} \cdot \nabla H_z + k^2 H_z = 0 \tag{5}$$

For TM polarization we solve equation $\nabla^2 E_z + k^2(1 - \omega_\mathrm{p}^2/\omega^2)E_z = 0$ to obtain the total field E_z. Here, ω_p is plasma frequency. We consider the plasma covers to be magnetized by a constant external magnetic field H_0 applied in the z-direction the cyclotron frequency corresponding to which is ω_0 .Plasma is a quasi-neutral gas including electrons, ions and molecules. Here we do not consider the movement of ions (and therefore the plasma frequency ω_p is only related to electrons). Under this condition, the relative dielectric permittivity tensor $\varepsilon = \epsilon\varepsilon_0$ of the plasma layers is approximately given by:

$$\epsilon = \begin{pmatrix} \epsilon & -\mathrm{i}\alpha \\ \mathrm{i}\alpha & \epsilon \end{pmatrix}$$

$$\epsilon = 1 - \frac{\omega_p^2}{\omega^2 - \omega_0^2} \tag{6}$$

$$\alpha = \frac{\omega_p^2(\frac{\omega_0}{\omega})}{\omega^2 - \omega_0^2}$$

In order to realize the investigated configuration and enclose the plasma, two metal cylinders with a radius of $0.5\,cm$ separated by a distance of $4\,cm$ are considered. Each rod is surrounded by a dielectric tube (chamber) with an approximate radius of $1\,cm$. The wall of the chamber is thin and transparent to radio waves and microwaves. Ideally, a material with a dielectric constant close to air should be chosen; however, a quartz tube with a very small thickness (e.g., less than $1\,mm$) is easily accessible and causes minimal disturbance to the microwave propagation considered in this work. It should be noted that the exact length of the antenna is not critical here, as our calculations and the permittivity tensor are based on the assumption that the antenna length is much larger than its radius (2D approximation). Therefore, a length of $40 - 50\,cm$ or more fulfills this condition. The air inside the tubes is evacuated, and argon gas is introduced. By controlling the gas flow, the pressure is maintained in the range of $10^{-3} - 1\,Torr$. In this pressure range, using an RF power supply of about $10\,W$, it is possible to achieve a charged particle density of the order of $n_e \approx 10^{10}\,cm^{-3}$. Naturally, increasing the power enhances the plasma density and, consequently, the plasma frequency. In typical laboratory plasmas, charged particle densities range from 10^9 to $10^{16}\,cm^{-3}$, corresponding to plasma frequencies of $f_\mathrm{p} = 10^9 - 10^{12}$ Hz [30, 31]. For consistency between the chosen frequency and plasma parameters, it should be noted that at 10 GHz a plasma density of the order of $10^{12}\,\mathrm{cm}^{-3}$ is required to satisfy $\omega_p/\omega \approx 0.9$. In laboratory conditions with pressures of $10^{-3} - 1$ Torr and RF power supplies of about $10\,W$, plasma densities in the range $10^{10} - 10^{12}\,\mathrm{cm}^{-3}$can realistically be achieved. This correction ensures that the physical parameters used in the model are consistent with practical plasma antenna and stealth applications.

Regarding the inhomogeneity of the plasma layer, it is worth noting that in practical scenarios such as electric discharge in free air (atmospheric pressure) a non-uniform plasma layer naturally forms around high-voltage electrodes. The ionization intensity, and thus the plasma density, decreases radially with distance from the cylinder. While our simulation focuses on the low-pressure collisionless regime, this physical behavior justifies the use of a radially decaying density profile ($n(r)$) in our theoretical model.

Eq. 5 is accompanied by the boundary condition $-n\varepsilon^{-1} \cdot \nabla H_z = q|_C$ related to continuity of tangential component of the electric field E_t at the fictitious boundary C. In this boundary condition, the left-hand-side of the equation, i.e. $-n\varepsilon^{-1} \cdot \nabla H_z$, is the tangential electric field E_t when r goes to the fictitious boundary C from the outside, but the right-hand-side of the equation, i.e. q, is the tangential electric field E_t when r goes to the fictitious boundary C from the inside. If the dielectric permittivity tensor ε has discontinuity but there is no surface source at the boundary of discontinuity, then H_z and $-n\varepsilon^{-1}\cdot\nabla H_z$ will be continuous on such a boundary. For TM polarization E_z and $-nE_z$ will be continuous on such a boundary. It is well-known from the variational principles for electromagnetics that the solution H_z of Eq. 5 under the boundary condition $-n\varepsilon^{-1}\cdot\nabla H_z = q|_C$ can be obtained by minimizing the functional (see chapter 6 of Ref. [32] for more details);

$$\mathcal{F}(H_z) = \oint_S ds\,(\nabla H_z^*\varepsilon^{-1}\cdot\nabla H_z - k^2|H_z|^2) + \oint_C dl\,(qH_z^* + q^*H_z) \quad (7a)$$

So, we discretize the region S into N_e small triangular elements and the functional $\mathcal{F}(H_z)$ in the region S is written as

$$\mathcal{F}(H_z) = \sum_{e=1}^{N_e}\mathcal{F}^{(e)}(H_z) \quad (7b)$$

where $\mathcal{F}^{(e)}(H_z)$ is the functional for eth triangular element. Now, we expand the solution H_z in the eth triangular element, i.e. H_z^e, in terms of the linear interpolation functions $\psi^{e,i}(r)$ as follows;

$$H_z^e = \sum_{i=1}^{3}\psi^{e,i}(r)\,H_z^{(e,i)} \quad (7c)$$

where $H_z^{(e,i)}$, the coefficients of the expansion, shows the value of H_z in the ith vertex of the eth triangular element. Here, the linear interpolation functions $\psi^{e,i}(r)$ is equal to one at the ith vertex of the eth triangular element and is equal to zero at the two other vertices of the eth triangular element. We substitute Eq. 7c in Eq. 7b to obtain the expansion of the functional $\mathcal{F}(H_z)$ in terms of the unknown coefficients $H_z^{(e,i)}$, then by setting to zero the variation of the resulting equation, we achieve the following system of linear equations;

$$\left(\frac{\epsilon M + \mathrm{i}\alpha K}{\varepsilon^2 - \alpha^2} - k^2N\right)H_z + Lq = 0 \quad (8)$$

In Eq. 8, the elements of a matrices M, K, and N are obtained by integrating of the interpolation functions $\psi^{e,i}(r)$ on the finite triangular elements in the region S. In addition, similar to Eq. 7c we expand the solution H_z in every finite boundary element at the fictitious boundary C. Substituting this expansion in the boundary integral equation, i.e. Eq. (3), leads to the following auxiliary system of equations;

$$(L+P)H_z + Qq = b \quad (9)$$

where the elements of a matrices L, P, and Q and the components of the column vector b are found by integrating of the interpolation functions on the finite boundary element at the fictitious boundary C. After numerically solving the system of Eqs. (8) and (9), unknown parameters H_z and q are obtained in region S and on the fictitious boundary C, respectively. In order to obtain the radar cross-section σ, we use the boundary integral equation i.e. Eq. (3) with $r' = Rn'$ to calculate H_z^{sc} at distances $r \longrightarrow \infty$ far from the rods. Due to the continuity of tangential electric field E_{t} namely $-n'\cdot\nabla' H_z = q|_C$ and the continuity of H_z on the fictitious boundary C, we have

$$\sigma = \lim_{r\to\infty} 2\pi r\frac{|H_z^{sc}|^2}{|H_z^{in}|^2} = \frac{1}{4k}\left|\oint_C dl'\,(k\hat{r}\cdot n'H_z(r') + \mathrm{i}q(r'))e^{-\mathrm{i}k\hat{r}\cdot(Rn')}\right|^2 \quad (10)$$

In the end of this section, it must be reminded that H_z and E_z individually satisfy the wave equation and it means that any solution to our problem can be regarded as the linear combination of two partial solutions $E_z = 0$, $H_z = 0$. Therefore, without loss of generality, investigation can be limited to these two cases. In fact, by identifying the equation solutions for TE and TM waves, the behavior of the system under a generic polarization is determined.

3. Numerical results

In this section, by considering the interaction between electromagnetic waves with double metallic rod system covered by inhomogeneous anisotropic plasma, determine the radar cross-section (RCS) and field profile to find the scattering and absorption characteristics of present configuration. In calculating RCS of this structure that can supposed as an antenna exposed by EM waves we use the FE-BI method applying formulas (1) to (10). The changes in the scattering pattern and the field profile of the configuration are caused by varying characteristics of the plasma cover.

Due to the anisotropy in the structure, the characteristics of the incident wave, especially the incident angle, are effective on RCS and the field profile.

In Figure (2), the real part of the total H_z field has been plotted for normalized plasma frequency $\omega_{\mathrm{p}}/\omega = 0.9$ and normalized cyclotron frequency $\omega_0/\omega = 1.5$. The profile of the electromagnetic fields corresponding to the parameters of Figure (2) is drawn for the TE polarization, and the effect of incidence angle and wavelength of the incident wave on the axial magnetic field of the total wave can be seen.

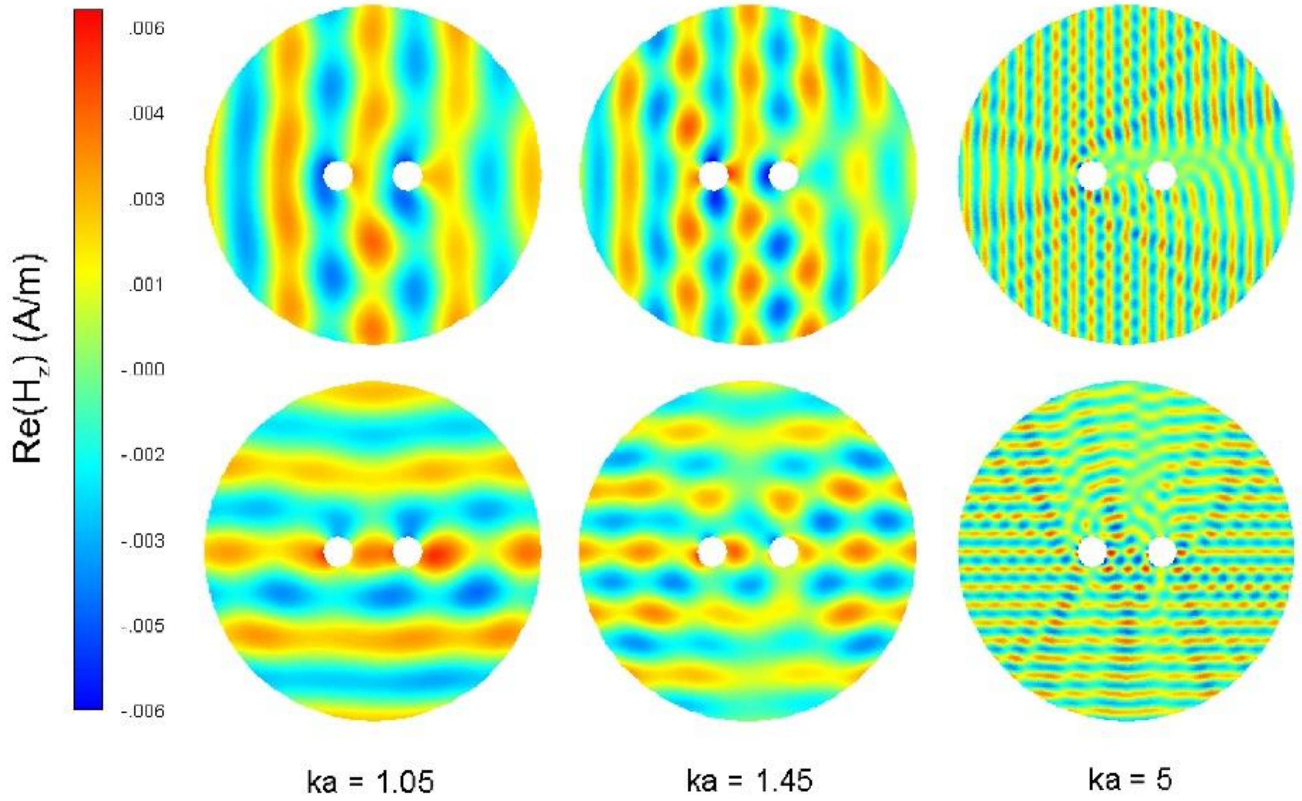

Figure 2. Panels in the first and second rows are for the incidence direction $\theta_0 = 0°$ and $\theta_0 = 90°$, respectively, with the wave numbers ka increasing from left to right panels. The vertical axis represents the real part of the magnetic field H_z (A/m)

In Figure (3), the radar cross-section $\sigma(\theta)$ has been plotted as a function of the scattering direction θ for incidence wave TE, when the plasma frequency is $\omega_p/\omega = 0.9$ and the incidence direction is $\theta_0 = 0°$. The solid lines show $\sigma(\theta)$ in the absence of the external magnetic field H_0 (The light solid lines show $\boldsymbol{\sigma}(\theta)$ when there is no plasma cover and give us the possibility of a comparison with cases that covered by plasma). The dashed lines show $\sigma(\theta)$ in the presence of the external magnetic field $\omega_0/\omega = 1.5$. The panels a1, a2, and a3 in the first column of Fig. (3) are for $\beta = 1$, where the density of the plasma cover on the metal columns has an inhomogenous distribution in the radial direction. The panels b1, b2, and b3 in the second column of Figure (3) are for parameter $\beta = 0$, where plasma covers of the structure have a homogenous density at thickness L from the edge of the metal columns. In both panels a and b of Figure (3), the wave numbers ka increase from up to down. As seen from Figure (3), the presence of an anisotropic plasma layer in the antenna disturbs symmetry of the radar cross-section pattern of the system. The absence of plasma or the presence of an isotropic even if inhomogeneous plasma, the symmetry of the scattered wave and as a result the scattering cross-section, are preserved. The solid lines show $\sigma(\theta)$ in the absence of the external magnetic field H_0 (The light solid lines show $\sigma(\theta)$ when there is no plasma cover and give us the possibility of a comparison with plasma covered cases). The dashed lines show $\sigma(\theta)$ in the presence of the external magnetic field $\omega_0/\omega = 1.5$. The panels a1, a2, and a3 in the first column of Figure (3) are for the incidence direction $\beta = 1$ with the wave numbers ka increasing from up to down panels. The panels b1, b2, and b3 in the second column of Figure (3) are for the incidence direction $\beta = 0$ with the wave numbers ka increasing from up to down panels.

Figure (4) shows the radar cross-section $\sigma(\theta)$ in terms of scattering angle θ for incidence wave TE, when the incidence direction is $\theta_0 = 90°$. Other parameters are as the same as in Figure (3). As expected, the symmetry of the radar cross-section is seen with respect to angle $\theta = \pi/2$ when the external magnetic field is zero or there is no plasma cover. In general, it can be seen from graphs (3) and (4) that if there is no plasma cover, the wave power is scattered in all directions with relatively low fluctuations. The presence of plasma cover around the metal columns concentrates the scattered wave energy in a specific direction.

This property makes it possible to use the present structure to amplify the wave in a preferred direction or as a plasma lens. As found from Figures (3) and (4) two factors anisotropy and inhomogeneity of the plasma layer can be effective in scattered wave distribution and scattering cross section.

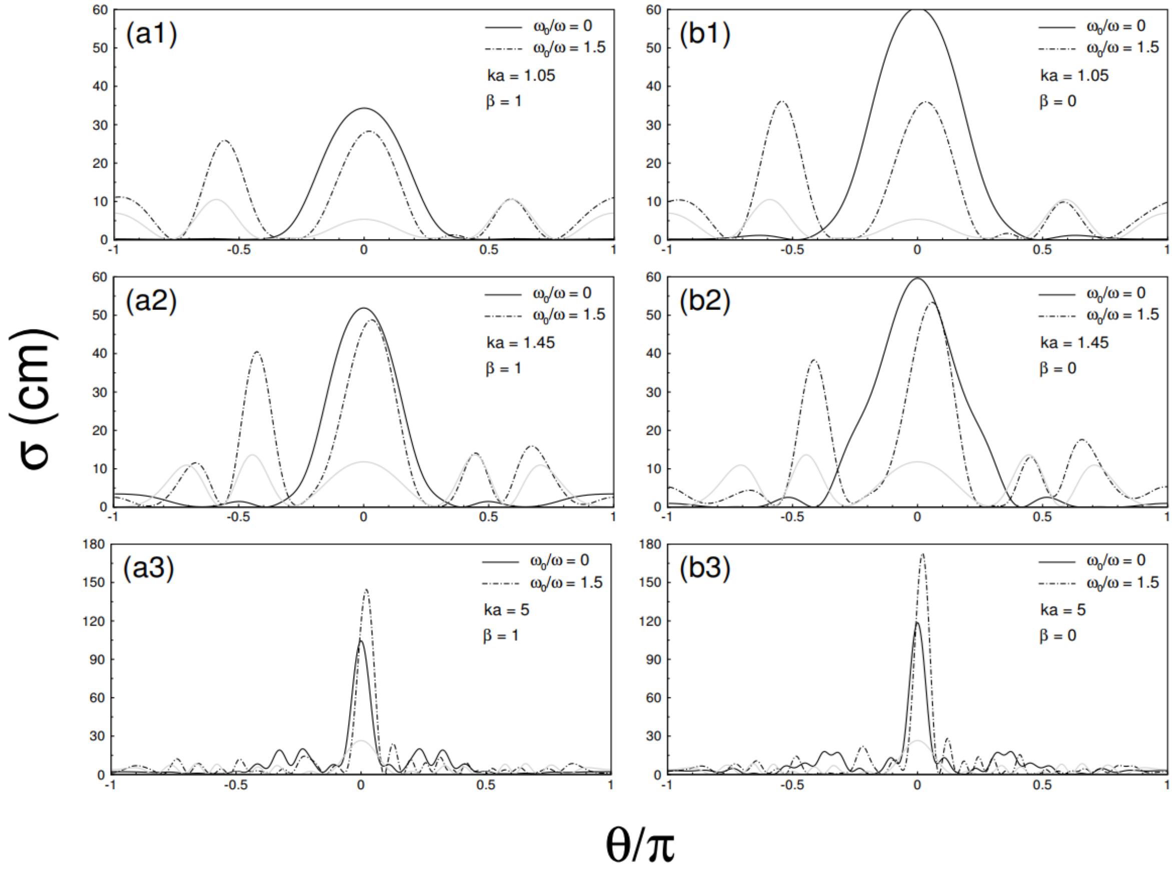

Figure 3. the radar cross-section $\boldsymbol{\sigma}(\theta)$ has been plotted as a function of the scattered direction θ for incident wave TE. Here, the plasma frequency is $\omega_p/\omega = 0.9$ and the incidence direction is $\theta_0 = 0°$

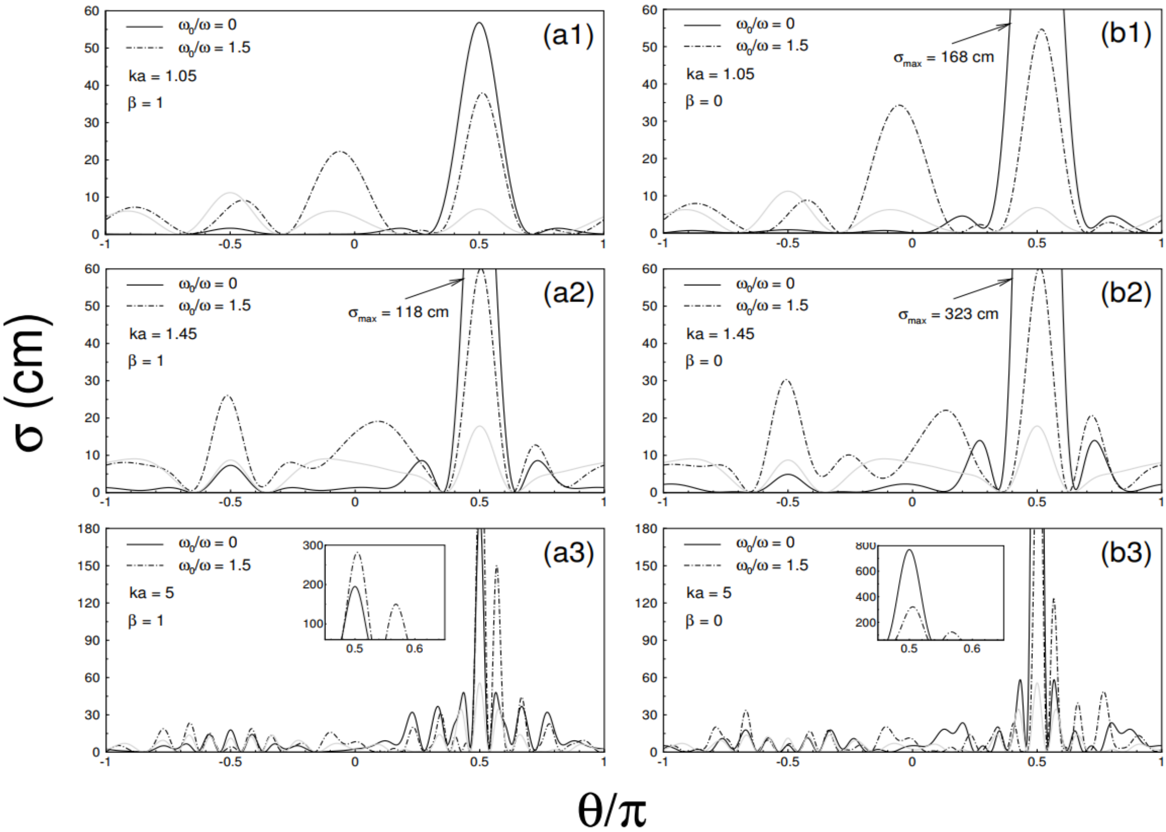

Figure 4. the radar cross-section $\sigma(\theta)$ has been plotted as a function of the scattered direction θ for incident wave TE with the incidence angle $\theta_0 = 90°$. Other parameters are as the same as in Figure (3)

If the external magnetic field is zero, the energy concentration is stronger and the main peak of the scattering cross-section is more intense than the lateral peaks. The presence of a magnetized plasma cover, in addition to breaking the symmetry, reduces the difference between the main and secondary peaks, and this effect is stronger for larger incident wavelengths. In general, the increase of the wave number in all the cases shown in Figures (3) and (4) has led to an increment in the scattering cross-section. The presence of plasma layer, especially homogeneous plasma whose density is maximum in the entire thickness of the layer, strengthens the mentioned effects. For example by increasing the wave number, in the conditions where there is no plasma cover (light solid lines), the scattering cross-section increment is not significant.

The reason of investigating the inhomogeneous plasma cover in the present work is that it is very difficult or even impossible to operationally create a plasma layer with uniform density around a metal without any physical boundary, such as a dielectric wall. In practical applications, plasmas produced in the laboratory or even space vehicles passing through the Earth's atmosphere where the air around them is ionized and a kind of plasma coating is created, the plasmas are non-uniform and their density varies from a maximum value to zero.

In Figure (5) the radar cross-section of incidence waves TM has been drawn for the same parameters as Fig. (3). As mentioned earlier, in the case of transverse magnetic field polarization, TM, the external magnetic field and its magnitude do not affect the results; so in Figure (5), only the influence of the existence of homogeneous $\beta = 0$ and inhomogeneous $\beta = 1$ plasma layers in the double metallic rod structure for different wave numbers has been seen. It should be noted that graphs are coincide in absence and presence of the external magnetic field $\omega_0/\omega = 1.5$. As expected for the incident wave TM, the scattering cross section is completely symmetrical.

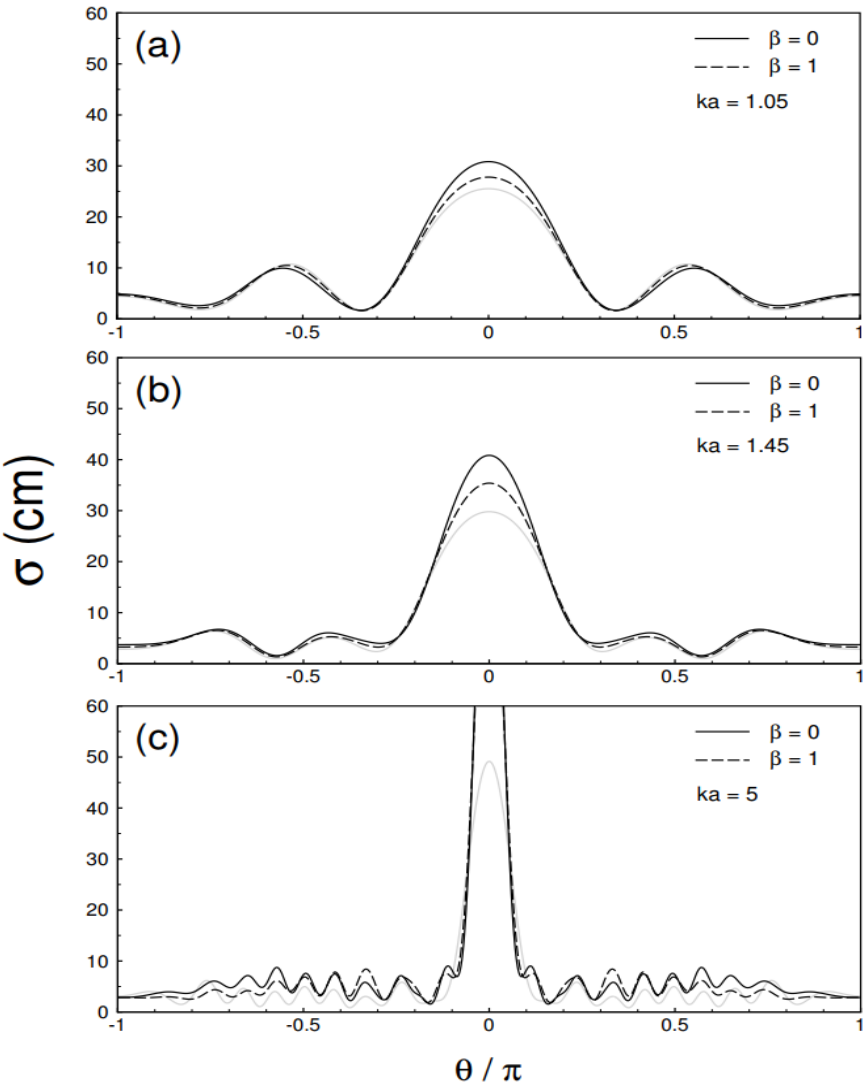

Figure 5. the radar cross-section $\sigma(\theta)$ has been plotted as a function of the scattered direction θ for incident wave TM with wave numbers ka increasing from up to down panels. Here the plasma frequency is $\omega_p/\omega = 0.9$ and the incidence direction is $\theta_0 = 0°$. The dashed lines show $\sigma(\theta)$ for parameter $\beta = 0$, and solid lines present $\sigma(\theta)$ for parameter $\beta = 1$ in the absence and presence of the external magnetic field with $\omega_0/\omega = 1.5$

The graphs match in the presence and absence of the external magnetic field. The light solid lines show $\sigma(\theta)$ when there is no plasma cover and give us the possibility of a comparison with plasma covered.

The physical interpretation of these results can be summarized as follows. First, the increase of RCS with larger values of ka is due to the shorter wavelength of the incident wave, which enhances constructive interference and resonance effects around the rods, leading to stronger scattering. Second, the presence of an inhomogeneous plasma layer reduces RCS in certain directions because the gradual radial variation of plasma density provides a smoother impedance transition, thereby decreasing reflections compared to a homogeneous plasma coating. Finally, the difference between TE and TM polarizations originates from the role of the external magnetic field. For TE waves, the magnetic field interacts with the plasma electrons through the Lorentz force, modifying the dielectric tensor and altering the scattering pattern. For TM waves, the electric field is aligned with the rod axis and does not couple to the axial magnetic field, so the scattering remains unaffected.

This point that the scattering of TE electromagnetic wave is affected by the static magnetic field, is due to the effect of the Lorentz force, and as a result intensity of the external magnetic field can be a controlling factor of the scattering pattern. If the wave polarization is TM, applying an external magnetic field in the axial direction has no effect on the intensity distribution of scattered field and radar cross-section of the system. In order to investigate the effect of the incidence angle more precisely, the scattering cross sections of the waves TE with different wavelengths from the two rod structure covered by inhomogeneous magnetized plasma layers $\omega_0/\omega = 1.5$, $\beta = 1$ have been drawn for two angles of incidence $\pi/6$ and $\pi/3$ in Figure (6).

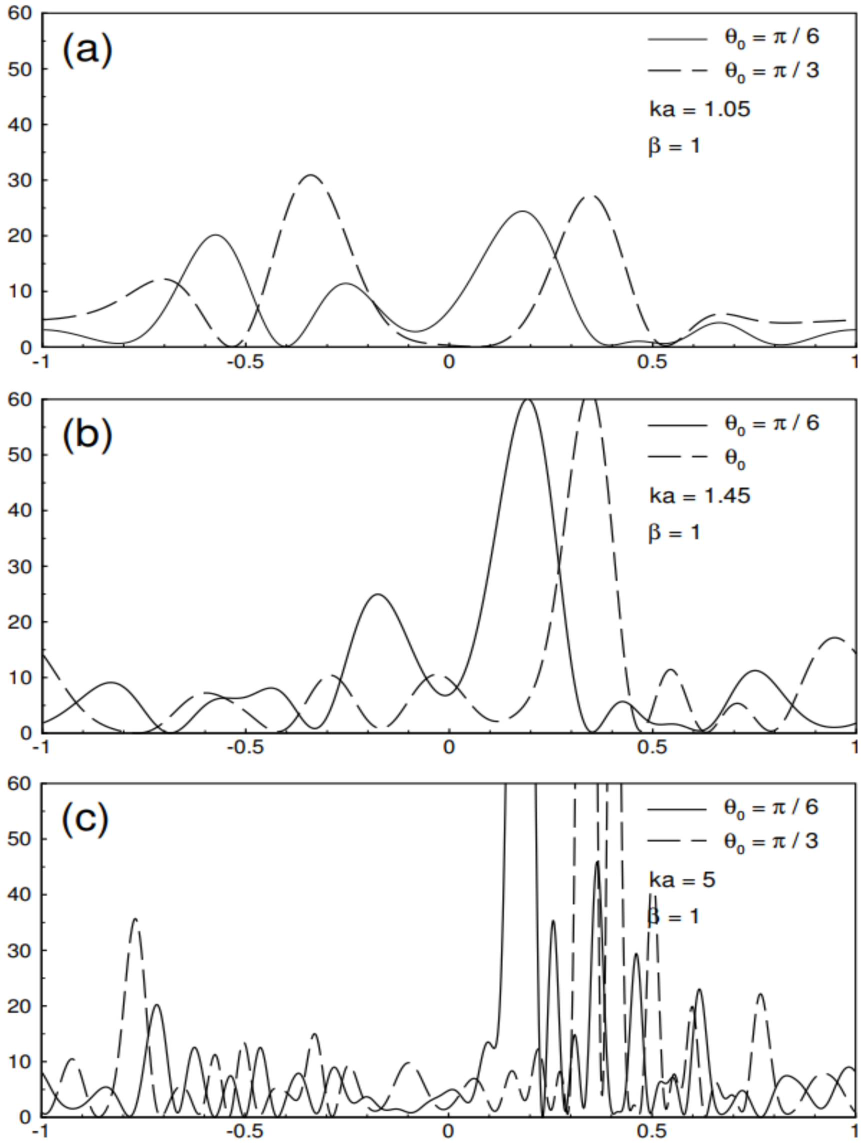

Figure 6. the radar cross-section $\sigma(\theta)$ has been plotted as a function of the scattered direction θ for incident wave TE with the incidence angles $\theta_0 = 30°, 60°$. Other parameters are as the same as in Figure (3)

10.57647/jtap.2026.2005.01

The landing angle of wave has a significant effect on the scattered field distribution and consequently on the radar cross-section as seen from Figure (6) in comparison with Figures (3), (4). Ultimately, we investigate the backscattering radar cross section (BRCS) of the configuration. Examining this characteristic of the system is a suitable tool in diagnostic processes and can provide useful information about the geometric dimensions and electromagnetic characteristics of the material that makes up the target object (or antenna). The graphs drawn in Figure (7) show that with increasing the wave number of incident wave, inhomogeneity of the plasma layer decreases BRCS of the system. However, for the wave number $ka = 1.05$, the difference between the BRCS in two homogeneous and inhomogeneous states is not significant.

As expected with decreasing wavelength, the fluctuations in BRCS increase.

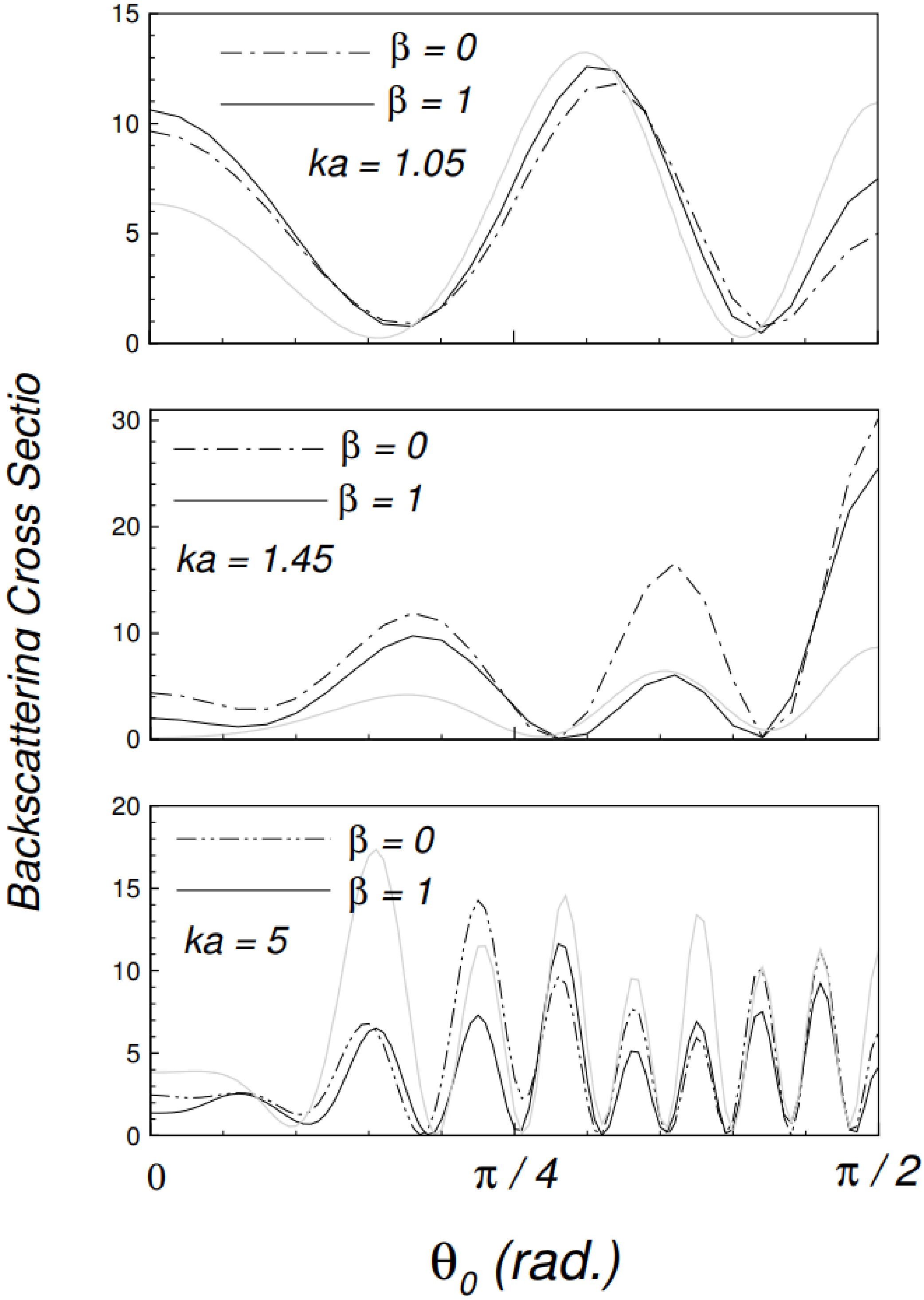

Figure 7. BRCS $\sigma_b(\theta)$ has been plotted as a function of the incident angle θ_0 when the cyclotron frequency is $\omega_0/\omega = 1.5$. Other parameters are as the same as in Figure (3)

4. Results and discussion

In this work, we investigated the scattering of electromagnetic waves with linear polarization from a double metallic rod system covered by an inhomogeneous plasma layer under a limited static magnetic field. The finite element boundary integral method was employed to obtain the profile of the total axial magnetic field due to the incidence of non-ionizing waves around the structure. The backscattering cross-section and scattering patterns were simulated for incident waves with different wavelengths and compared with cases without plasma coating or with homogeneous plasma layers.

The role of the static magnetic field in modifying the dielectric tensor of plasma and its interaction with the anisotropic plasma-metal structure was carefully considered

The numerical results presented in Part III demonstrated that the scattering cross-section depends on the presence of plasma, the density profile of the plasma layer, its isotropy or anisotropy, the wavelength, and the polarization of the incident electromagnetic wave.

The investigations of the influence of external magnetic field intensity on scattering characteristics and electromagnetic field profiles provide a compelling exploration of how magnetized plasma coatings can influence the scattering and concealment of objects.

The observed impact of the static magnetic field, particularly affecting the scattering of electromagnetic waves in the case of TE polarization, underscores the significance of the Lorentz force in altering wave propagation within the antenna–plasma system.

The collisionless plasma assumption adopted in this work is justified by the physical parameters of the modeled system. With ratio $\frac{\upsilon}{\omega} \approx 10^{-4}$ to 10^{-3}, collisions are negligible and the resulting expression provides an excellent approximation to the accurate value.

5. Conclusion

In this study, the electromagnetic scattering from a double metallic rod system covered by inhomogeneous anisotropic plasma layers was investigated using the Finite Element-Boundary Integral (FE-BI) method. The numerical results demonstrate that the scattering characteristics are strongly dependent on the plasma density profile, the external magnetic field, and the polarization of the incident wave. Specifically, it was found that radial inhomogeneity in the plasma layer acts as a graded-index impedance matching medium, effectively reducing the Radar Cross Section (RCS) and Backscattering RCS (BRCS) compared to homogeneous coatings.

Furthermore, the application of an external static magnetic field introduces anisotropy that breaks the symmetry of the scattering pattern for TE polarization due to the Lorentz force interaction, while TM polarization remains unaffected.

Consequently, the proposed configuration offers a highly tunable platform where scattering can be either suppressed for stealth and concealment purposes or enhanced for directional signal transmission in satellite communications.

Authors Contribution

All the authors have participated sufficiently in the did all simulations and compiled the manuscript, as well as the writing of the manuscript.

Availability of data and materials

All data presented in this article are available on request.

Conflict of interests

The authors declare that there is no conflict of interest to this work.

References

[1] Caorsi S., Pastorino M., Raffetto M. Analytic SAR computation in a multilayer elliptic cylinder for bioelectromagnetic applications. Bioelectromagnetics: Journal of the Bioelectromagnetics Society, the Society for Physical Regulation in Biology and Medicine, the European Bioelectromagnetics Association. 1999;20(6):365–371. https://doi.org/10.1002/(SICI)1521-186X(199909)20:6<365::AID-BEM5>3.0.CO;2-G

[2] Kourosdari N., Shaterian Z., Karami Horestani A. Transparent antenna technology and its application in space. Technology in Aerospace Engineering. 2020;4(2): 35–44. https://doi.org/20.1001.1.26764253.1399.4.2.4.4

[3] Monti A., Soric J., Barbuto M., Ramaccia D., Vellucci S., Trotta F., Alù A., Toscano A., Bilotti F. Mantle cloaking for co-site radio-frequency antennas. Applied Physics Letters. 2016;108(11). https://doi.org/10.1063/1.4944042

[4] Alù A., Engheta N. Cloaking a sensor. Physical Review Letters. 2009;102(23):233901. https://doi.org/10.1016/j.metmat.2010.03.005

[5] Wu X. B., Yasumoto K. Three-dimensional scattering by an infinite homogeneous anisotropic circular cylinder: an analytical solution. Journal of Applied Physics. 1997;82(5):1996–2003. https://doi.org/10.1063/1.366009

[6] Rappaport C. M., McCartin B. J. FDFD analysis of electromagnetic scattering in anisotropic media using unconstrained triangular meshes. IEEE Transactions on Antennas and Propagation. 1991;39(3):345–349. https://doi.org/10.1109/8.76332

[7] Chen H., Cheng D. Scattering of electromagnetic waves by an anisotropic plasma-coated conducting cylinder. IEEE Transactions on Antennas and Propagation. 1964;12(3):348–353. https://doi.org/10.1109/TAP.1964.1138206

[8] Adey A. W. Scattering of electromagnetic waves by coaxial cylinders. Canadian Journal of Physics. 1956;34(5):510–520. https://doi.org/10.1139/p56-057

[9] Ghaffar A., Yaqoob M., Alkanhal M. A., Ahmed S., Naqvi Q., Kalyar M. Scattering of electromagnetic wave from perfect electromagnetic conductor cylinders placed in un-magnetized isotropic plasma medium. Optik. 2014;125(17):4779–4783. https://doi.org/10.1016/j.ijleo.2014.04.061

[10] Shi W., Yuan B., Mao J., Wang C. Enhancement of electromagnetic energy by plasma antenna. Nano Energy. 2020;76:105053. https://doi.org/10.1016/j.nanoen.2020.105053

[11] Borg G. G., Harris J. H., Miljak D. G., Martin N. M. Application of plasma columns to radiofrequency antennas. Applied Physics Letters. 1999;74(22):3272–3274. https://doi.org/10.1063/1.123317

[12] Jaafar H., Ali M. T. B., Dagang A. N. B., Zali H. M., Halili N. A. A reconfigurable monopole antenna with fluorescent tubes using plasma windowing concepts for 4.9-GHz application. IEEE Transactions on Plasma Science. 2015;43(3):815–820. https://doi.org/10.1109/TPS.2015.2398878

[13] Golharani S., Heidari-Semiromi E., Jazi B., Rahmani Z. Plasma-covered long cylindrical non-isotropic dielectric lenses for targeted control of energy distribution. The European Physical Journal Plus. 2020;135(9):1–12. https://doi.org/10.1140/epjp/s13360-020-00791-0

[14] Kumar R., Bora D. Wireless communication capability of a reconfigurable plasma antenna. Journal of Applied Physics. 2011;109(6). https://doi.org/10.1063/1.3564937

[15] Zhao J., Wang S., Wu H., Liu Y., Chang Y., Chen X. Flexible plasma linear antenna. Applied Physics Letters. 2017;110(9). https://doi.org/10.1063/1.4977952

[16] Yeh C., Kaprielian Z. Scattering from a cylinder coated with an inhomogeneous dielectric sheath. Canadian Journal of Physics. 1963;41(1):143–151. https://doi.org/10.1139/p63-013

[17] Stratigaki L., Ioannidou M., Chrissoulidis D. Scattering from a dielectric cylinder with multiple eccentric cylindrical dielectric inclusions. IEE Proceedings Microwaves, Antennas and Propagation. 1996;143(6):505–511. https://doi.org/10.1049/ip-map:19960854

[18] Foroutan V. Numerical study of the homogeneous and inhomogeneous magnetic field effects on the plasma-based radar cross-section reduction. IET Radar, Sonar & Navigation. 2020;14(3):468–476. https://doi.org/10.1049/iet-rsn.2019.0318

[19] Rao Z., Zhu G., He S., Li C., Yang Z., Liu J. Simulation and analysis of electromagnetic scattering from anisotropic plasma-coated electrically large and complex targets. Remote Sensing. 2022;14(3):764. https://doi.org/10.3390/rs14030764

[20] Geng Y., Wu X., Li L.-W. Analysis of electromagnetic scattering by a plasma anisotropic sphere. Radio Science. 2003;38(6):1–12. https://doi.org/10.1029/2003RS002913

[21] Ghaffar A., Yaqoob M., Alkanhal M. A., Sharif M., Naqvi Q. Electromagnetic scattering from anisotropic plasma-coated perfect electromagnetic conductor cylinders. AEU—International Journal of Electronics and Communications. 2014;68(8):767–772. https://doi.org/10.1016/j.aeue.2014.03.001

[22] Naito T., Tanaka T., Fukuma Y., Sakai O. Electromagnetic wave cloaking and scattering around an antiresonance-resonance symmetrical pair in the frequency domain. Physical Review E. 2019;99(1):013204. https://doi.org/10.1103/PhysRevE.99.013204

[23] Monti A., Soric J., Alù A., Toscano A., Bilotti F. Design of cloaked Yagi-Uda antennas. EPJ Applied Metamaterials. 2016;3:10. https://doi.org/10.1051/epjam/2016012

[24] Ouyang W., Liu Y., Deng W., Zhang Z., Zhao C. Study of the electromagnetic wave propagation in realistic plasma. Microwave and Optical Technology Letters. 2020;62(2):660–668. https://doi.org/10.1002/mop.32091

[25] Qian J.-W., Zhang H.-L., Xia M.-Y., et al. Modelling of electromagnetic scattering by a hypersonic cone-like body in near space. International Journal of Antennas and Propagation. 2017;2017. https://doi.org/10.1155/2017/3049532

[26] Dutta R., Biswas R., Roy N. Reduction of attenuation of EM wave inside plasma formed during supersonic or hypersonic re-entry of missile like flight vehicles by the application of DC magnetic field—a technique for mitigation of RF blackout. In: 2011 IEEE Applied Electromagnetics Conference (AEMC). IEEE; 2011. p. 1–4. https://doi.org/10.1109/AEMC.2011.6256917

[27] Dolph C. L., Weil H. On the change in radar cross-section of a spherical satellite caused by a plasma sheath. Planetary and Space Science. 1961;6:123–132. https://doi.org/10.1016/0032-0633(61)90012-5

[28] Kirichenko Y. V. Cylindrical plasma antenna with large longitudinal density irregularity. Journal of Communications Technology and Electronics. 2018;63:438–445. https://doi.org/10.1134/S1064226918050042

[29] Kirichenko Y. V. Radiation from a plasma layer with a strong longitudinal irregularity. Journal of Communications Technology and Electronics. 2017;62:1367–1374. https://doi.org/10.1134/S1064226917110079

[30] Alexandrov A. F., Bogdankevich L. S., Rukhadze A. A., et al. Principles of plasma electrodynamics. Vol. 9. Springer; 1984. https://doi.org/10.1007/978-3-642-69247-5

[31] Krall N. A., Trivelpiece A. W., Gross R. A. Principles of plasma physics. American Journal of Physics. 1973;41(12):1380–1381. https://doi.org/10.1119/1.1987587

[32] Jin J.-M. The finite element method in electromagnetics. John Wiley & Sons; 2015. ISBN: 1118842022; 9781118842027.

[33] Magarotto L., Neto A. G., Albani M. Plasma antennas: a comprehensive review. IEEE Access. 2024;12:45123–45145. https://doi.org/10.1109/ACCESS.2024.3411142

[34] Maquet J., Guillon P., André F. ANSYS HFSS as a new numerical tool to study wave propagation inside anisotropic magnetized plasmas. arXiv preprint arXiv:2305.11234. 2023. https://doi.org/10.1007/s12044-025-00842-5

[35] Zhang Y., Li K., Wang T. Mechanical and corrosion properties of plasma-sprayed Fe-based amorphous/nanocrystalline composite coating. Advances in Materials and Processing Technologies. 2019;5(2):145–158. https://doi.org/10.1080/2374068X.2019.1598129

[36] Khalil Sh. M., Mousa N. M. Dispersion characteristics of plasma-filled cylindrical waveguide. Journal of Theoretical and Applied Physics. 2014;8(1):1–14. https://doi.org/10.1007/s40094-014-0111-2

[37] Golian Y., Dorranian D. Proton driven plasma wakefield generation in a parabolic plasma channel. Journal of Theoretical and Applied Physics. 2017;11(1):27–35. https://doi.org/10.1007/s40094-016-0235-7

[38] Saviz S., Salehizadeh F. Plasma effect in tape helix traveling-wave tube. Journal of Theoretical and Applied Physics. 2014;8(2):125. https://doi.org/10.1007/s40094-014-0125-9

[39] Miraboutalebi S., Rajaei L., Khadivi Borogeni M. K. Plasmon resonance coupling in cold overdense dissipative plasma. Journal of Theoretical and Applied Physics. 2013;7(1):24. https://doi.org/10.1186/2251-7235-7-24